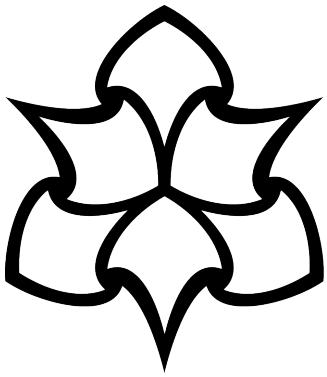

A novel genetic variant in *PTGS1* affects N-glycosylation of cyclooxygenase-1 causing a dominant–negative effect

Verónica Palma-Barqueros[1,#], Marilena Crescente[2,#], María Eugenia de la Morena[1], Melissa V Chan[2,3], Elena Almarza[4], Nuria Revilla[1], Natalia Bohdan[1], Antonia Miñano[1], José Padilla[1], Harriet E Allan[2], Tania Maffucci[5], Matthew L. Edin[6], Darryl. C. Zeldin[6], Cristina Mesa-Nuñez[4], Carlos Damian[4], Ana Marín-Quilez[7], Rocío Benito[7], Irene Martínez-Martínez[1], Nuria Bermejo[8], Ignacio Casas-Aviles[8], Agustín Rodríguez Alen[9], José Ramón González-Porras[10], Jesús María Hernández-Rivas[7,10], Vicente Vicente[1], Javier Corral[1], María Luisa Lozano[1], Timothy D. Warner[2], *José María Bastida[10,11], & *José Rivera[1,11]

[1]Servicio de Hematología y Oncología Médica, Hospital Universitario Morales Meseguer, Centro Regional de Hemodonación, Universidad de Murcia, IMIB-Arrixaca, CIBERER-U765, Murcia, Spain

[2]Centre for Immunobiology, Blizard Institute, Barts and the London School of Medicine and Dentistry, Queen Mary University London, 4 Newark Street, London, E1 2AT, United Kingdom

[3]The National Heart, Lung, and Blood Institute's Framingham Heart Study, Framingham, Massachusetts, USA

[4]Division of Hematopoietic Innovative Therapies, Centro de Investigaciones Energéticas Medioambientales y Tecnológicas (CIEMAT)/Centro de Investigación Biomédica en Red de Enfermedades Raras (CIBERER) and Advanced Therapies Unit, Instituto de Investigación Sanitaria Fundación Jiménez Díaz (IIS-FJD/UAM). Madrid, Spain

[5]Centre for Cell Biology and Cutaneous Research, Blizard Institute, Barts and The London School of Medicine and Dentistry, Queen Mary University of London, London, UK

[6]National Institutes of Health, National Institute of Environmental Health Sciences, Research Triangle Park, North Carolina, USA

[7] IBSAL, IBMCC, CIC, Universidad de Salamanca-CSIC, Salamanca, Spain

[8]Servicio de Hematología, Hospital San Pedro de Alcántara, Complejo Universitario de Cáceres, Cáceres, Spain

[9]Servicio de Hematología y Hemoterapia, Hospital Virgen de la Salud, Complejo Hospitalario de Toledo, Spain.

[10] Departamento de Hematología, Hospital Universitario de Salamanca, Salamanca-IBSAL

[11]On behalf of the "Grupo Español de Alteraciones Plquetarias Congénitas, (GEAPC)"; Hemorrhagic Diathesis Working Group, SETH.

#These authors contributed equally to this work. *These authors share senior authorship.

Correspondence:

José Rivera, Centro Regional de Hemodonación-Universidad de Murcia, Ronda de Garay s/n, Murcia 30003, Spain. Phone: +34-968-341990; Fax: +34-968-261914; e-mail: jose.rivera@carm.es

Counts

Main Text: 1727 words

Figures: 1

References: 15

Supplemental Figures: 5

Supplemental Tables: 4

Running Head. New COX-1 defect due to altered N-Glycosylation

Keywords: *PTGS1*, COX-1 deficiency, inherited platelet disorders, N-glycosylation, bleeding disorders.

Key Points

- A novel genetic variant, p.Asn143Ser, in COX-1 was identified in heterozygosity in a patient with lifelong moderate bleeding diathesis
- This mutation disrupts N-Glycosylation of COX-1 and causes an aspirin-like platelet dysfunction with a dominant-negative effect

To the editor

During platelet activation, arachidonic acid (AA) is released from membrane phospholipids and metabolized to thromboxane A_2 (TXA_2) through the actions of cyclooxygenase-1 (COX-1) and TXA_2 synthase. TXA_2 binds to the platelet TXA_2 receptor, causing shape change, secretion and platelet aggregation.[1] COX-1 (599aa; 70kDa) has cyclooxygenase and peroxidase activities and it is functionally active as a homodimer, with each COX-1 monomer consisting of four highly conserved domains: an N-terminal signal peptide, a dimerization domain, a membrane-binding domain (MBD) and a large C-terminal catalytic domain[2] (**Figure 1A**). Irreversible COX-1 inhibition by aspirin is a widely established anti-platelet therapy in cardiovascular disease.[3]

Despite the physiological and clinical relevance of platelet COX-1, few patients with congenital COX-1 defect (Bleeding Disorder Platelet Type 12; OMIM: 605735) have been characterized[2]. In the 1970's some patients with mild bleeding diathesis, impaired aggregation and blunted TXA_2 synthesis were described, but with no genetic confirmation. To date, only a few cases with uncommon genetic variants in *PTGS1*, the gene encoding COX-1*,* have been reported, without detailed study of their associated platelet phenotype. A patient with severe bleeding carried the *PTGS1* single nucleotide polymorphisms (SNPs) p.Arg8Trp and p.Pro17Leu.[2] Heterozygosity for the p.Pro17Leu SNP also aggravated hemorrhage in a pedigree with hemophilia A.[2] Another patient showing bleeding and reduced TXA_2 synthesis was heterozygous for the rare *PTGS1* variant c.337C>T (p.Arg113Cys) and the common variant c.1003G>A (p.Val481Ile).[2] Recently, the BRIDGE Consortium reported a pedigree with an autosomal recessive variant c.965G>C (p.Trp322Ser) that abrogated COX-1 expression resulting in aspirin-like platelet dysfunction.[4]

Here, we report a patient presenting with a lifelong mild bleeding tendency and platelet dysfunction, associated to heterozygosity for the novel *PTGS1* variant c.428A>G (p.Asn143Ser). The distinguished feature of this mutation is that it disturbs one N-glycosylation sequon at the catalytic domain of COX-1 causing the expression of a dysfunctional hypo-glycosylated COX-1 protein with an apparent dominant-negative effect. The methodological details of this investigation are provided in **Supplemental Material.**

The proband was a 13-year-old teen from Asiatic origin, adopted by a Spanish family, presenting with a lifelong moderate bleeding diathesis (bruising and petechiae, being more frequent after minor traumas; recurrent epistaxis sometimes associated to nonsteroidal anti-inflammatory drug (NSAIDs) intake; menorrhagia, once requiring tranexamic acid and desmopressin treatment; excessive bleeding after surgical procedures such as tonsillectomy)(ISTH-BAT=6). On repeated testing, she showed normal blood cell counts including platelet number and volume (**Supplemental Table 1**) and no visible abnormalities in blood smears. Blood biochemical and coagulation parameters were within normal ranges. No clinical signs of relevant organ/tissue, immune or cognitive dysfunction were present. Detailed platelet phenotyping was performed that showed: i) PFA-100 closure times slightly and pathologically extended for collagen/ADP and collagen/epinephrine cartridges, respectively (**Supplemental Table 1)**; ii) normal expression of major platelet adhesive receptors (**Supplemental Figure 1A**); iii) fibrinogen binding was reduced by about 50% in proband´s platelets stimulated with several agonists but PAR4 (**Supplemental Figure 1B**); iv) impaired agonist-induced α- (10-30%) and δ- (25-50%) granule secretion, as evaluated by measurement of P-selectin and CD63 expression (**Supplemental Figure 1C**); v) light transmission aggregometry confirmed an aspirin-like platelet dysfunction in the proband, characterized by normal aggregation in response to PAR1p and ristocetin, and reduced aggregation with ADP and collagen (**Supplemental Figure 1D)**. Moreover, the proband's platelets showed absent AA-induced aggregation, but normal aggregation to U46619, a stable TXA_2 analog, indicating unaffected signaling downstream the TXA_2 receptor (**Figure 1B**); vi) markedly reduced platelet synthesis of TXA_2 in the supernatant of the LTA experiments (<10% of the control levels) (**Supplemental Figure 2A)**; and vii) reduced synthesis of all COX-1-dependent eicosanoids in whole blood stimulated with collagen or PAR1p **(Supplemental Figure 2B)(Supplemental Table 2).** Overall, this clinical and platelet phenotype resembles that of the few previously reported cases with COX-1 defect.[2]

Analysis of proband's DNA with a HTS-gene panel,[5] revealed an heterozygous variant c.428A>G (p.Asn143Ser) in the exon 5 of the *PTGS1* gene (ENST00000362012), which was confirmed by Sanger sequencing. The proband's biological parents were not available to assess the inheritance pattern of the variant. This variant is not reported in

gnomAD or 1000 genomes project databases, but a c.429C>G [p.Asn143Lys] change is listed in the gnomAD collection with a very low allele frequency of $3.98x10^{-6}$. As highlighted in **Figure 1A**, the novel p.Asn143Ser substitution is located at the N-terminal of the COX-1 catalytic domain and affects a highly conserved residue (Genomic Evolutionary Rate Profiling conservation score=5.59; https://varsome.com/) (**Supplemental Figure 3A).** Remarkably, Asn143 is one of the three predicted N-glycosylation sites in COX-1 (**Figure 1A**). The recent and firstly resolved human COX-1 crystal by Scilimati A *et al*. (https://www.rcsb.org/structure/6Y3C) (**Supplemental Figure 3B**) confirmed that Asn143 is decorated by an N-glycan chain. Changing Asn to Ser would theoretically abolish this N-glycosylation resulting in an hypo-glycosylated protein with unknown consequences in folding, secretion, stability and enzymatic activity. Following the ACMG standards, the current verdict for the p.Asn143Ser variant is of Uncertain Significance, despite most computational analysis *in silico* predict a deleterious effect (https://varsome.com/) (**Supplemental Table 3**).

Immunofluorescence analysis of platelets and leukocytes showed no apparent impairment in COX-1 expression in the proband (**Supplemental Figure 4**). However, 8% SDS–PAGE of platelet lysates and immunoblotting analysis revealed a second COX-1 protein band with lower molecular weight in the proband, which is consistent with the predicted hypo-glycosylated COX-1 variant **(Figure 1C)**. In contrast to these findings, a recent study has showed that recessive inheritance of the 965G>C (p.Trp322Ser) missense variant in *PTGS1,* results in loss of COX-1 platelet expression instead of COX-1 loss-of function.[4]

Strong evidence of the deleterious effect of p.Ans143Ser variant in COX-1 glycosylation and its enzyme activity was obtained in HEK 293 T cells transfected with either wild-type (Asn143) or mutated (Ser143) enzyme vector (**Supplemental Table 4**). In this cell model, the variant Ser143 COX-1 displayed higher electrophoretic mobility than wild-type Asn143 COX-1, as was expected for a hypo-glycosylated enzyme with reduced molecular mass. Moreover, cells co-transfected with both Asn143 and Ser143 COX-1**,** simulating heterozygosis status, had a COX-1 double protein band similar to that observed in patient´s platelet lysates (**Figure 1D**). Importantly, this COX-1 double band disappeared upon treatment of the lysates from co-transfected cells with N-glycosidase F (**Figure 1E**). As shown in **Figure 1F,** cells expressing wild-type COX-1

(Asn143) responded to 500 μM AA stimulation with a notable TXB_2 production whilst cells transfected with mutant Ser143 COX-1 displayed almost no TXB_2 synthesis (194±48.2 pg/mL), resembling untransfected cells (UNT) (169.0±24.8 pg/mL). Interestingly, cells co-transfected with equal amounts of wild-type (Asn143) and mutant Ser143 COX-1 (1.5 μg of each vector) showed 70% reduced TxB2 synthesis in comparison to cells transfected with 1.5 μg of wild-type COX-1 vector (Asn143+Ser143, 907.5±888.9 pg/mL vs. Asn143, 2906.9±3736.1) (**Figure 1F**). These results were confirmed in a separate series of experiments in which cells transfected with Asn143 COX-1 vector (1.5 or 3 μg) produced TXB_2 in a dose-dependent manner when stimulated with increasing concentrations of AA (0.5-10 μM), while in cells transfected with the mutant Ser143 this synthesis was abrogated. Remarkably, co-transfected cells (Asn143+Ser143) displayed higher than 50% reduction in TXB_2 synthesis as compared to cells solely transfected with an equivalent dose of Asn143 COX-1 (**Figure 1G**). These data strongly support that the p.Ans143Ser variant has a dominant-negative effect in COX-1 activity. To further test this, we established a second model in which HEK 293 cells were first stably transfected with either mutant Ser143 or wild-type Asn143 COX-1, and then they were transiently transfected with the alternative construct. The TXB_2 synthesis was abolished in cells stably expressing Ser143 COX1 and co-expression of wild-type Asn143 COX-1 partially recovered TXB_2 production, but following a non-linear dose-dependent pattern (**Figure 1H**). Similar results were found in the opposite cell model (**Supplemental Figure 5**). Noteworthy, introduction in HEK 293 T cells of a different mutation, p.Ser145Ala, disrupting the same consensus N-glycosylation sequence (Asn-X-Ser/Thr) in COX-1, also resulted in null AA-induced TXA_2 synthesis (**Figure 1F**) and in the expression of the hypo-glycosylated COX-1 protein also disappearing after treatment with N- glycosidase F (**Figure 1D-E**).

Overall, these results obtained in the patient platelets and in transfected cells reflected that the p.Asn143Ser variant has a dominant-negative effect and its deleterious action exceeded that of simply haploinsufficiency of functional COX-1 protein. Since COX-1 is active as a homodimer, we can speculate that a mechanism contributing for such a dominant negative effect is an impaired activity of both wild-type/mutant and mutant/mutant dimers. Indeed, dimerization of glycosylated and non-glycosylated monomers of COX-2, an isoform of COX-1, has been reported and this is more

energetically favorable than the dimerization between two N-glycosylated monomers.[6] Additionally, it may also be possible that the loss of N-glycans reduces the steric hindrance favoring the access of AA into the catalytic domain of the non-functional mutant COX-1, as suggested by the blunted TXA_2 synthesis, at low AA concentration, in cells co-transfected with equivalent levels of mutant Ser143 COX-1 and wild-type COX-1. Of note, a similar dominant negative mechanism has been described for the London variant of antithrombin.[7]

To our knowledge, three N-glycosylation sequons are predicted in human COX-1 at positions 67, 143 and 409,[8] and the recent resolution of a human COX-1 crystal structure by Scilimati *et al.* (PDB:6y3) provided the first experimental evidence that Asn143 is decorated by an N-glycan chain. Our results demonstrate, for the first time, that the N-glycosylation at 143 is functionally relevant as its disruption, by mutation of Asn143 or Ser145 residues, results in a smaller and dysfunctional COX-1 variant. In agreement with our results, Otto *et al.*[9] has demonstrated that ovine COX-1 is N-glycosylated at positions Asn68, Asn144 and Asn410, the orthologous residues to the human ones, and removal of these N-glycans also abolishes the cyclooxygenase and peroxidase activity of hypo-glycosylated ovine COX-1 mutants.[9]

Mechanistically, glycans can influence protein folding, cellular trafficking and secretion, substrate binding affinity, proteolysis or clearance and the catalytic activity of proteins[10]. Indeed, the relevance of glycosylation in the function of proteins of the haemostatic system such as FXI,[11,12] antithrombin,[13] VWF[10], protein S[14] or the platelet P2Y12 ADP receptor,[15] has been shown.

In summary, this work extends the genetic spectrum of COX-1 defects, by the characterization of a patient with a novel variant c.428A>G in *PTGS1*. Studies performed on the patient's platelets and in cell models showed that this variant affects the post-transductional COX-1 N-glycosylation and leads to expression of a hypo-glycosylated protein with a dominant-negative effect in COX-1 enzymatic activity. COX-1 hypo-glycosylation is unveiled as a new dominant-negative mechanism causing congenital platelet function disorder. More broadly, our study strengthens the relevance of N-glycans in human health and disease.

Authorship Contributions

VPB, MC, MEM, MVC, EA, NB, AM, JP, AMQ and JR performed platelet function studies. VPB, MEM, EA, CM, CD, JCC and IM participated in cell models design and assays. MC, MVC, HEA, TF and TDW did TXA2 measurements, cell immunostaing and immunoblotting. MLE and DCZ performed eicosanoid measurements and analysis. NB and ICA recruited the patient and perform clinical management. NR, ARA, NB, ICA, VVG, MLA, JMB and JR examined clinical data. VPB, RB, JRGP, JMHR, JMB & JR performed and assessed molecular studies. VPB, MC, TDW, MLA, JMB and JR wrote the manuscript. All authors helped in data interpretation and critically reviewed the paper.

Disclosure of Conflicts of Interest

The authors declare no conflict of interest. The views expressed in this manuscript are those of the authors and do not necessarily represent the views of the National Heart, Lung, and Blood Institute; the National Institutes of Health; or the U.S. Department of Health and Human Services.

Funding and Acknowledgements

This work was partially supported by grants from Instituto de Salud Carlos III (ISCIII) & Feder (PI17/01311, PI20/00926, PI18/00598, PI17/01966 and CB15/00055), Fundación Séneca (19873/GERM/15), Gerencia Regional de Salud (GRS 2061A/19 and 1647/A/17), Fundación Mutua Madrileña (FMM, AP172142019) and Sociedad Española de Trombosis y Hemostasia (SETH-FETH; Premio López Borrasca 2019 and Ayuda a Grupos de Trabajo en Patología Hemorrágica). TDW research is supported by a grant from the British Heart Foundation (PG/17/40/33028). VPB has predoctoral contract from CIBERER. MEMB has a postdoctoral contract from University of Murcia. AMQ holds a predoctoral grant from the Junta de Castilla y León.

The corresponding author research on Inherited Platelet Disorders is conducted in accordance with the aims of the Functional and Molecular Characterization of Patients with Inherited Platelet Disorders Project, which is supported by the Hemorrhagic

Diathesis Working Group of the Spanish Society of Thrombosis and Haemostasis (SETH).

ORCID

Veronica Plama-Barqueros : http://orcid.org/0000-0002-5699-0053

Marilena Crescente, https://orcid.org/0000-0003-3164-512X

Timothy D Warner, https://orcid.org/0000-0003-3988-4408

José María Bastida, https://orcid.org/0000-0002-8007-3909

José Rivera, http://orcid.org/0000-0003-4225-6840

References

1. Rivera J, Lozano ML, Navarro-Nunez L, Vicente V. Platelet receptors and signaling in the dynamics of thrombus formation. *Haematologica*. 2009;94(5):700-711.

2. Palma-Barqueros V, Bohdan N, Revilla N, Vicente V, Bastida JM, Rivera J. PTGS1 gene variations associated with bleeding and platelet dysfunction. *Platelets*. 2020:1-7.

3. Collaborative meta-analysis of randomised trials of antiplatelet therapy for prevention of death, myocardial infarction, and stroke in high risk patients. *BMJ*. 2002;324(7329):71-86.

4. Chan MV, Hayman MA, Sivapalaratnam S, et al. Identification of a homozygous recessive variant in PTGS1 resulting in a congenital aspirin-like defect in platelet function. *Haematologica*. 2020.

5. Bastida JM, Lozano ML, Benito R, et al. Introducing high-throughput sequencing into mainstream genetic diagnosis practice in inherited platelet disorders. *Haematologica*. 2018;103(1):148-162.

6. Vann-Victorino DDC, Cunanan J, Chen M, Chan R, Hall RW, Sevigny MB. Effect of glycosylation of cyclooxygenase-2 (COX-2) on homodimerization. *The FASEB Journal*. 2017;31(S1):lb79-lb79.

7. Raja SM, Chhablani N, Swanson R, et al. Deletion of P1 arginine in a novel antithrombin variant (antithrombin London) abolishes inhibitory activity but enhances heparin affinity and is associated with early onset thrombosis. *J Biol Chem*. 2003;278(16):13688-13695.

8. Majed BH, Khalil RA. Molecular mechanisms regulating the vascular prostacyclin pathways and their adaptation during pregnancy and in the newborn. *Pharmacol Rev*. 2012;64(3):540-582.

9. Otto JC, DeWitt DL, Smith WL. N-glycosylation of prostaglandin endoperoxide synthases-1 and -2 and their orientations in the endoplasmic reticulum. *J Biol Chem*. 1993;268(24):18234-18242.

10. Preston RJS, Rawley O, Gleeson EM, O'Donnell JS. Elucidating the role of carbohydrate determinants in regulating hemostasis: Insights and opportunities. *Blood*. 2013;121(19):3801-3810.

11. McVey JH, Lal K, Imanaka Y, Kemball-Cook G, Bolton-Maggs PH, Tuddenham EG. Characterisation of blood coagulation factor XI T475I. *Thromb Haemost*. 2005;93(6):1082-1088.

12. Linssen M, Mohamed M, Wevers RA, Lefeber DJ, Morava E. Thrombotic complications in patients with PMM2-CDG. *Mol Genet Metab*. 2013;109(1):107-111.

13. de la Morena-Barrio ME, Martínez-Martínez I, de Cos C, et al. Hypoglycosylation is a common finding in antithrombin deficiency in the absence of a SERPINC1 gene defect. *Journal of Thrombosis and Haemostasis*. 2016;14(8):1549-1560.

14. Denis CV, Roberts SJ, Hackeng TM, Lenting PJ. In vivo clearance of human protein S in a mouse model: influence of C4b-binding protein and the Heerlen polymorphism. *Arterioscler Thromb Vasc Biol*. 2005;25(10):2209-2215.

15. Zhong X, Kriz R, Seehra J, Kumar R. N-linked glycosylation of platelet P2Y12 ADP receptor is essential for signal transduction but not for ligand binding or cell surface expression. *FEBS Letters*. 2004;562(1-3):111-117.

Legend to Figures

Figure 1. The novel *PTGS1* variant p.Asn143Ser affecting the N-glycosylation residue 143 in COX-1, results in aspirin- like impaired platelet aggregation and expression of a hypo-glycosylated and dysfunctional COX-1 enzyme in human platelet and cell models.

A) Schematic representation for COX-1 showing the different domains and the localization of the novel p.Asn143Ser genetic variant as well as all previously reported common (dotted blue lines) and rare (dotted red lines) variants. N-glycosylated residues are highlighted in grey circles. **B)** Platelet aggregation in response to arachidonic acid and U46619, a TxA2 analog, was evaluated in PRP from the proband (black dotted line) and from two healthy controls (grey dotted line and black line). **C)** Two independent western blots representing COX-1 in platelets from the proband and time-matched control. Platelet lysates were resolved in 8% SDS- polyacrylamide gel for 90 min. In addition to wild-type COX-1 (black arrow), a second COX-1 band with lower molecular weight (red arrow) was detected in the patient. Grey arrow identified a non-specific band. β-actin was used as an internal control. **D)** Western blot determination of COX-1 expression in 293 T HEK cells untransfected (UNT), transfected with wild-type Asn143 COX-1 vector (Asn143), mutant Ser143 COX-1 vector (Ser143), co-transfected with both vectors (Asn143+Ser143), or transfected with mutant Ala145 COX-1 vector (Ala145), β-actin was used as an internal control. **E)** Western blots of COX-1 expression in untransfected (UNT) or variant transfected 293 T HEK cells treated (+) or not (-) with N-glycosidase F. **F)** 293 T HEK cells were untransfected (UNT), transfected with wild-type Asn143 COX-1 vector (Asn143), mutant Ser143 COX-1 vector (Ser143), co-transfected with both vectors (Asn143+Ser143), or transfected with mutant Ala145 COX-1 vector (Ala145). The enzymatic activity of COX-1 was then assessed by using ELISA for TXB_2 to assess the formation of TXA_2 following incubation with 500 μM arachidonic acid. Plots show mean plus standard deviation from values obtained in three 3 independent experiments. "*" denotes P value=0.05 vs. Asn143 (U de Mann-Whitney test). **G)** 293 T HEK cells untransfected (UNT), transfected with different amounts of wild-type Asn143 COX-1 vector, transfected with mutant Ser143 COX-1 vector, or co-transfected with the same amount of both vectors (Asn143+Ser143),

were stimulated with different concentrations of AA (0.5 -10 μM) and the formation of TXA_2 was assessed by using ELISA. The plot is representative of 2 independent experiments. **H)** HEK 293 cells were transfected with vector expressing Ser143 mutant COX-1 and the neomicine resistance gen and grown in the presence of geneticine. Resistant and stable transfected cell clones were isolated and then transfected with different amounts of vector (0-1 μg) expressing native Asn143 COX-1. Cells were washed and split for preparation of protein lysates and for arachidonic acid (1 μM) stimulation and TXA_2 production measurement by ELISA. A double COX-1 protein is seen in co-transfected cells. Native COX-1 recovers TXA_2 production, but following a non-linear dose-dependent pattern.

Figure 1

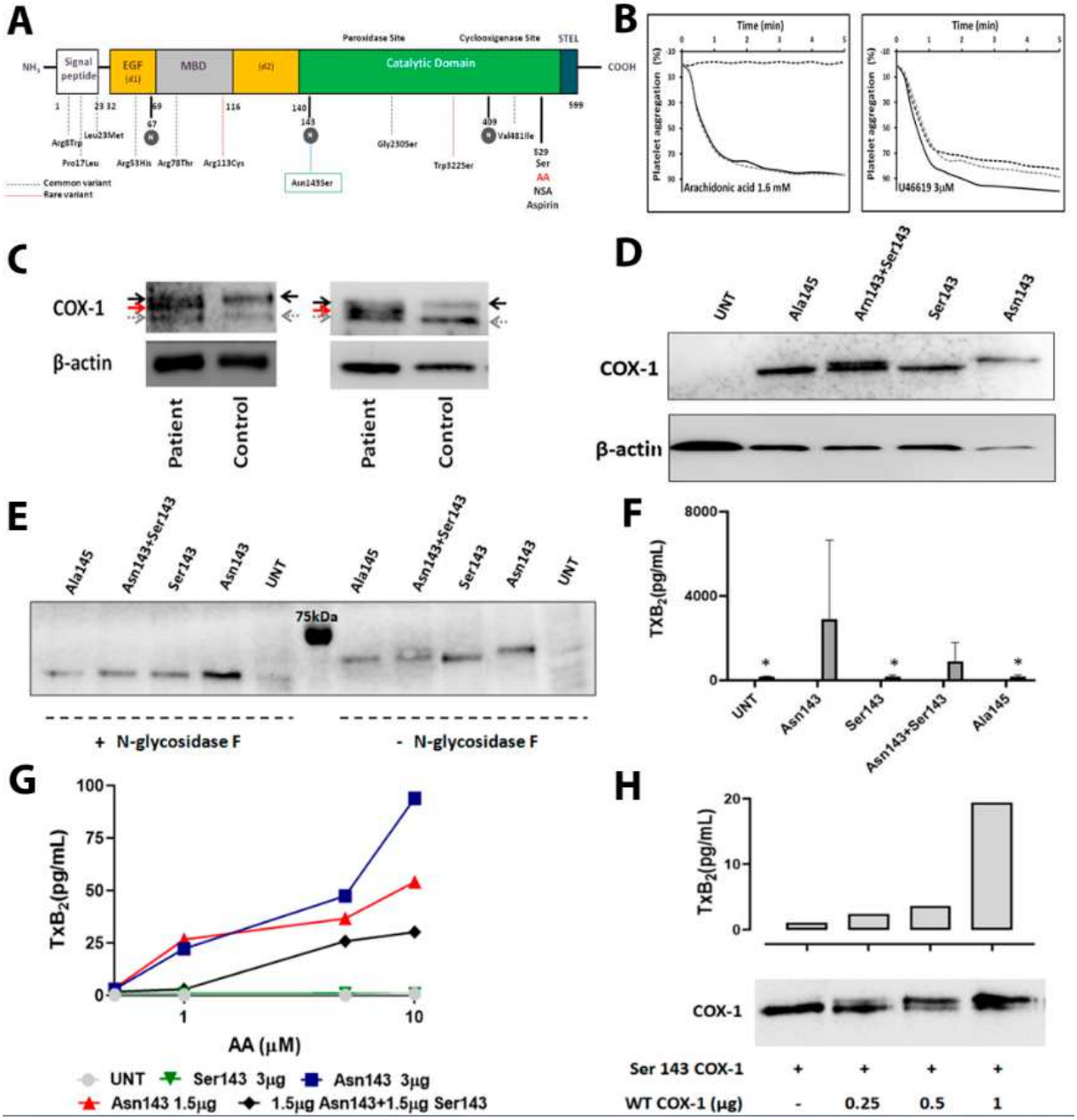
A
Signal peptide
EGF
MBD
Catalytic Domain
Peroxidase Site
Cyclooxigenase Site
STEL
COOH
Arg6Trp
Pro17Leu
Leu23Met
Arg53His
Arg78Thr
Arg113Cys
Asn143Ser
Gly230Ser
Trp322Ser
Val481Ile
E29 Ser
AA
NSA
Aspirin
Common variant
Rare variant
B
Time (min)
Platelet aggregation (%)
Arachidonic acid 1.6 mM
U46619 3μM
C
COX-1
β-actin
Patient
Control
Patient
Control
D
UNT
Ala145
Arn143+Ser143
Ser143
Asn143
COX-1
β-actin
E
Ala145
Asn143+Ser143
Ser143
Asn143
UNT
Ala145
Asn143+Ser143
Ser143
Asn143
UNT
75kDa
+ N-glycosidase F
- N-glycosidase F
F
TXB2(pg/mL)
8000
4000
0
UNT
Asn143
Ser143
Asn143+Ser143
Ala145
G
TxB2(pg/mL)
100
75
50
25
0
1
10
AA (μM)
UNT
Ser143 3μg
Asn143 3μg
Asn143 1.5μg
1.5μg Asn143+1.5μg Ser143
H
TxB2(pg/mL)
20
10
0
COX-1
Ser 143 COX-1
WT COX-1 (μg)
+
+
+
+
-
0.25
0.5
1

A novel genetic variant in *PTGS1* affects N-glycosylation of cyclooxygenase-1 causing a dominant–negative effect

Verónica Palma-Barqueros *et al.*

Supplemental Material

Patients, blood sampling, and DNA collection

The proband was a 13-year-old teen from Asiatic origin adopted by a Spanish family, who was enrolled in the Spanish multicenter project "Functional and Molecular Characterization of Patients with Inherited Platelet Disorders".[1,2] This project followed the Helsinki Declaration and had the approval of the Ethics Committees of the Instituto de Investigación Biomédica (IBSAL, Salamanca, Spain) and Hospital Universitario Reina Sofía (Murcia, Spain). The patient, and control subjects, provided written informed consent. Clinical data were reviewed by the investigator team and bleeding symptoms were scored using ISTH bleeding assessment tool (ISTH-BAT).[3,4]

Venous blood was drawn into either 7.5% K3 EDTA tubes (for complete blood counts [CBC] and DNA purification) or buffered 0.105 M sodium citrate (for functional studies). CBC were performed using a Sysmex® XS1000i hematological counter (Sysmex España, Spain). DNA was isolated using a DNeasy blood and tissue kit, (Qiagen, Germany) and quantified using a Qubit 2.0 fluorometer (ThermoFisher Scientific, CA, USA).

Molecular analysis by HTS gene panel and Sanger sequencing

The patient DNA was analysed by high-throughput sequencing (HTS)-gene panel using a MiSeq Illumina platform (Illumina, CA, USA).[2,5] The identified genetic variants were assessed according to the standards of the American College of Medical Genetics and Genomics and the Association for Molecular Pathology (ACMG).[6] The PTGS1 variant identified in the index case by HTS-gene panel[2] was confirmed by means of Sanger sequencing in an ABI 3130 automated sequencer. The following specific forward and reverse primers were designed using Primer3 (http://bioinfo.ut.ee/primer3/)

PTGS1 5F: cttgtcaccgttatttttgctctct

PTGS1 5R: atctgtaaagacccaaacacagaga

Genomic DNA was amplified with the Fast Start High Fidelity PCR System (Roche, Basel, Switzerland) following the manufacturer's instructions, with some variations in the annealing temperature. DNA sequences were evaluated using Chromas Lite v2.1.1 (Technelysium, South Brisbane, Australia) and DS Gene v1.5 (Accerlys, San Diego, CA) software. Data were analyzed using annotations of genome version hg19/GRCh37. COX-1 sequence alignment with 12 species was done by using Uniprot and visualized with Jalview software.[7] The new human COX-1 crystal structure (https://www.rcsb.org/structure/6Y3C) was visualized in the Chimera software (UCSF, CA, USA).

Platelet aggregation

Platelet-rich-plasma (PRP) and platelet poor plasma (PPP) from citrate whole blood were prepared by stepwise centrifugation (140 × g, 15 min; 1000 × g, 10 min, respectively). Light transmission aggregometry (LTA) in PRP (2 x 10^{11} platelets/L) was performed as described[1] by using an Aggrecorder II aggregometer (Menarini Diagnostics, Florence, Italy). Time course changes in the maximal percentage of light transmission of PRP over baseline PPP were recorded for 300 seconds upon stimulation with the following platelet agonists: 1.6 mM arachidonic acid [AA; Sigma-Aldrich, UK], 10 µM ADP [Chronolog, UK], 10 µg/ml Collagen [Nycomed, Austria], 25 µM protease-activated receptor agonist peptide (PAR1p) (TRAP-6; Bachem, Austria], 10 µM U46619 (Cayman Chemical, UK) and 1.25 mg/mL Ristocetin [Helena Bioscience, UK]

Platelet flow cytometry

Platelet expression of membrane glycoproteins (GPs) GPIa (integrin α2, CD49b), GPIbα (CD42B), GPIX (CD42Aa), GPIIb (integrin subunit αIIb, CD41a), GPIIIa (β3, CD61) and GPVI was evaluated by flow cytometry in citrated whole blood diluted 1:10 in sterile phosphate-buffered saline (PBS) using specific antibodies (all from BD Biosciences, Madrid, Spain). To analyze platelet granule secretion and $\alpha_{IIb}\beta_3$ activation, diluted PRP (~20 × 10^9/L platelets) was incubated under static conditions (30 minutes at room temperature [RT]) with Tyrode's buffer, as control for non-stimulated platelets, or with agonists in the presence of anti-CD41*APC (as a platelet marker), fibrinogen-Alexa488 (Thermo Fisher, Madrid, Spain) and anti-CD62*PE (α-granule secretion) or anti-

CD63*PE (dense granule secretion) (BD Biosciences). Reactions were stopped with 4% paraformaldehyde (PFA) (v/v) (15 min, RT), samples were diluted with PBS and then run in a BD Accuri™ C6 device (BD Biosciences, Ann Arbor, MI, USA). The median fluorescence intensity (MFI) of CD41a positively stained cells (platelets) was analysed using BD Accuri™ C6 software[8].

Platelet TXB_2 synthesis

LTA assays were stopped by adding 100 μmol/L diclofenac sodium (Sigma-Aldrich, UK) and 100 U/mL heparin (Leo Laboratories, UK). Samples were centrifuged (500 x g, 2 min) and supernatants were collected and stored at -80°C until TXB_2 measurement by ELISA (Cayman Chemical, MI, USA).

Eicosanomic profile in whole blood

Citrated whole blood was incubated with phosphate buffered saline (PBS), collagen (30 μg/mL) or PAP1p-6 (25μM) (37°C, 30 min) under stirring conditions in the aggregometer. Stimulation was ended with 100 μmol/L diclofenac sodium (Sigma-Aldrich, UK) and 100 U/mL heparin (Leo Laboratories, UK). Plasma supernatants (2000 x g, 5 min) were collected and stored frozen until use for total eicosanoids measurement by gas chromatography–tandem mass spectrometry as described elsewhere.[9,10] Briefly, after extraction with ethyl acetate, samples were passed through Maestro A columns (Tecan, Switzerland) under gravity flow, columns were washed with acetonitrile, samples were dried by vacuum centrifugation at 37°C and reconstituted in 30% ethanol. Platelet eicosanoids were then separated by reverse-phase HPLC on a 1 x 150 mm, 5 μm Luna C18 (2) column (Phenomenex, CA, USA) and quantified using an MDS Sciex API 3000 triple quadrupole mass spectrometer (Applied Biosystems-ThermoFisher Scientific) with negative-mode electrospray ionization and multiple reaction monitoring.

Immunofluorescence studies in platelets and leukocytes

The immunostaining of platelets and leukocytes was performed essentially as described before.[11] Briefly, platelet-rich-plasma was fixed with 4% paraformaldehyde in PBS at room temperature for 15 min. Then, platelets were washed with PBS-ACD (22.0 g/L citric acid, trisodium salt, dihydrate; 7.3 g/L citric acid, anhydrous; and 24.5

g/L D-(+)-Glucose), (pH 6.1,) and resuspended in 1% BSA (Sigma-Aldrich). For leukocyte analysis, the interface between PRP and red blood cells was separated, Lyse/Fix solution (BD Bioscience, Germany) was added and leukocytes were isolated by centrifugation (2000 x g, 5 min) and diluted in saline. Platelets or leukocytes were spotted onto glass coverslips at 37°C for 90 min and then blocked with the blocking buffer (0.2% Triton X-100, 2% donkey serum and 1% BSA) for 60 min. Following this, cells were incubated with anti-COX-1 (Cell Signaling Technology, UK; 4841S; 1:100), anti-α-tubulin (Sigma-Aldrich, T5168; 1:200) and anti-CD45 (Abcam, UK, ab8216; 1:200) antibodies overnight.

Cells were washed and incubated for 60 minutes with Alexa 647-conjugated secondary antibody (donkey anti-rabbit polyclonal IgG H+L; Life Technologies; A-31573; 1:500) and Alexa 488-conjugated secondary antibody (donkey anti-mouse polyclonal IgG H+L; Life Technologies; A-21202; 1:500) to detect COX-1, α-tubulin and CD45, respectively. Samples were incubated with DAPI (25 μg/mL; Life Technologies) for 10 minutes to stain leukocyte nuclei. The coverslips were then mounted onto glass slides and visualized with oil immersion objectives (CFI Plan Apochromat 40X, N.A.1.4, working distance 0.26 mm – 63x for platelets and 40x for leukocytes) on a confocal laser scanning microscope (LSM 880 with Airyscan, Zeiss, UK). Acquisition and image processing were performed using the ZEN software (Version 2.35spi, Zeiss) and ImageJ (Version 1.51a, National Institutes of Health, USA)

Cell models for mutant COX-1

To assess the effect of COX-1 genetic variants we established HEK 293T and HEK 293 cells models. These cells were selected as they hardly express COX-1.[12] pcDNA3.1+/C-(K)-DYK vectors containing wild-type or mutant (c.428A>G [p.Asn143Ser]) cDNA g of *PTGS1* were commercially available (OHu14933D, Genscript). A Ser145Ala construct was prepared by PCR-based site-directed mutagenesis on the commercial pcDNA3.1 wild-type vector, by using the Stratagene QuikChange Site-Directed Mutagenesis kit with appropriate primers as described.[13]

HEK 293T or HEK 293 cells (ATCC, LGC Standards S.L.U. Spain) were grown in Dulbecco's modified Eagle's medium (DMEM) containing 10% fetal bovine serum.

HEK 293 T cells (2 x 10^5 /well) were transiently transfected with vectors expressing wild-type or mutant (p.Arg143Ser or p.Ser145Ala) COX-1 using Lipofectamine 3000

(ThermoFisher Scientific). Comparable transfection efficiencies in either condition were ensured by flow cytometry measurement of intracellular levels of recombinant COX-1 using the BD IntraSure kit (BD Biosciences) and the antibody α-DYKDDDDK*PE (BioLegend, CA, USA, Cat#637309).

HEK 293 cells (2 x 10^5 /well) were transfected with vectors expressing wild-type (Asn143) or Ser143 mutant COX-1 as above, also containing the neomicine resistance gen. Cell were grown in a geneticine (G418, ThermoFisher Sicentific) containing media for 20 days. Resistant and stable transfected cell clones were isolated and grown separately. Finally, cells expressing either the wild-type or the Ser143 mutant COX-1 were transiently transfected with different amounts of vector (0.25-3 μg) expressing the alternative COX-1 protein.

In either case, at 48h post-trasnfection, cells were washed with PBS and splitted for the stimulation experiment and for preparation of protein lysates. In stimulation experiments, cells (25 x10^4 for each transfection condition) were incubated with PBS or 500 μM AA for 30min at 37 °C, centrifuged (5 min, 1000 x g) and the supernatants were recovered and stored frozen at -80°C until TXA_2 determination by ELISA (Cayman Chemical).

Western blot analysis

Standard western blotting procedures were used.[8] Briefly, washed platelets (1 × 10^9 platelets/mL) were resuspended in modified Tyrode's HEPES buffer (134 mmol/L NaCl, 2.9 mmol/L KCl, 0.34 mmol/L Na_2HPO_4, 12 mmol/L $NaHCO_3$ and 1 mmol/L $MgCl_2$ and 20mmol/L HEPES, pH 7.4; all Sigma, UK), pH 7.4, containing protease inhibitors (cOmplete™ Protease Inhibitor Cocktail, Sigma-Aldrich, UK) were lysed with Triton X-100 (0.5% v/v). Proteins were separated by 8% SDS–PAGE and transferred to polyvinylidene fluoride membranes. Blots, were stepwise incubated with primary antibodies against COX-1 and β-actin (Cell Signaling Technology, cat# 4841S and (Sigma-Aldrich, cat# A3854 respectively) followed by secondary horseradish peroxidase–conjugated goat anti-rabbit IgG antibody (Sigma-Aldrich, cat# 12-348).

Proteins were detected by chemiluminescence (ECL prime; GEHealthcare).For N-glycosylation analysis, lysates from cell transfections were denatured for 5 min at 100°C in 150 mM sodium phosphate buffer, pH 7.4, supplemented with 2% SDS and 1M β-mercaptoetanol.[14] Samples were chilled on ice and digested at 37°C for 15h with

0.6 U N-glycosidase F (PNGase-F, Roche Diagnostics GmbH, Germany) in the presence of 15% Triton X-100. Finally, cell proteins lysates, with or without N-glycosidase F treatment, were separated on 8% SDS-PAGE gels and immunoblotting was carried out as above.

Statistical analysis

All functional assays were performed in parallel with samples from the patient and from at least one healthy control. Unless specifically stated, statistical comparisons could not be performed because of the limited sample number.

References

1. Sanchez-Guiu I, Anton AI, Padilla J, et al. Functional and molecular characterization of inherited platelet disorders in the Iberian Peninsula: results from a collaborative study. *Orphanet J Rare Dis*. 2014;9:213.
2. Bastida JM, Lozano ML, Benito R, et al. Introducing high-throughput sequencing into mainstream genetic diagnosis practice in inherited platelet disorders. *Haematologica*. 2018;103(1):148-162.
3. Gresele P, Orsini S, Noris P, et al. Validation of the ISTH/SSC bleeding assessment tool for inherited platelet disorders: A communication from the Platelet Physiology SSC. *J Thromb Haemost*. 2020;18(3):732-739.
4. Rodeghiero F, Tosetto A, Abshire T, et al. ISTH/SSC bleeding assessment tool: a standardized questionnaire and a proposal for a new bleeding score for inherited bleeding disorders. *J Thromb Haemost*. 2010;8(9):2063-2065.
5. Lozano ML, Cook A, Bastida JM, et al. Novel mutations in RASGRP2, which encodes CalDAG-GEFI, abrogate Rap1 activation, causing platelet dysfunction. *Blood*. 2016;128(9):1282-1289.
6. Richards S, Aziz N, Bale S, et al. Standards and guidelines for the interpretation of sequence variants: a joint consensus recommendation of the American College of Medical Genetics and Genomics and the Association for Molecular Pathology. *Genet Med*. 2015;17(5):405-424.
7. Waterhouse AM, Procter JB, Martin DM, Clamp M, Barton GJ. Jalview Version 2--a multiple sequence alignment editor and analysis workbench. *Bioinformatics*. 2009;25(9):1189-1191.
8. Hardy AT, Palma-Barqueros V, Watson SK, et al. Significant Hypo-Responsiveness to GPVI and CLEC-2 Agonists in Pre-Term and Full-Term Neonatal Platelets and following Immune Thrombocytopenia. *Thromb Haemost*. 2018;118(6):1009-1020.
9. Edin ML, Hamedani BG, Gruzdev A, et al. Epoxide hydrolase 1 (EPHX1) hydrolyzes epoxyeicosanoids and impairs cardiac recovery after ischemia. *J Biol Chem*. 2018;293(9):3281-3292.
10. Newman JW, Watanabe T, Hammock BD. The simultaneous quantification of cytochrome P450 dependent linoleate and arachidonate metabolites in urine by HPLC-MS/MS. *J Lipid Res*. 2002;43(9):1563-1578.
11. Kahr WHA, Lo RW, Li L, et al. Abnormal megakaryocyte development and platelet function in Nbeal2(-/-) mice. *Blood*. 2013;122(19):3349-3358.

12. Sood R, Flint-Ashtamker G, Borenstein D, Barki-Harrington L. Upregulation of prostaglandin receptor EP1 expression involves its association with cyclooxygenase-2. *PloS one*. 2014;9(3):e91018-e91018.
13. Navarro-Fernandez J, Eugenia de la Morena-Barrio M, Martinez-Alonso E, et al. Biochemical and cellular consequences of the antithrombin p.Met1? mutation identified in a severe thrombophilic family. *Oncotarget*. 2018;9(69):33202-33214.
14. de la Morena-Barrio ME, Martinez-Martinez I, de Cos C, et al. Hypoglycosylation is a common finding in antithrombin deficiency in the absence of a SERPINC1 gene defect. *J Thromb Haemost*. 2016;14(8):1549-1560.

Supplemental Figure 1. The proband's platelet function phenotype

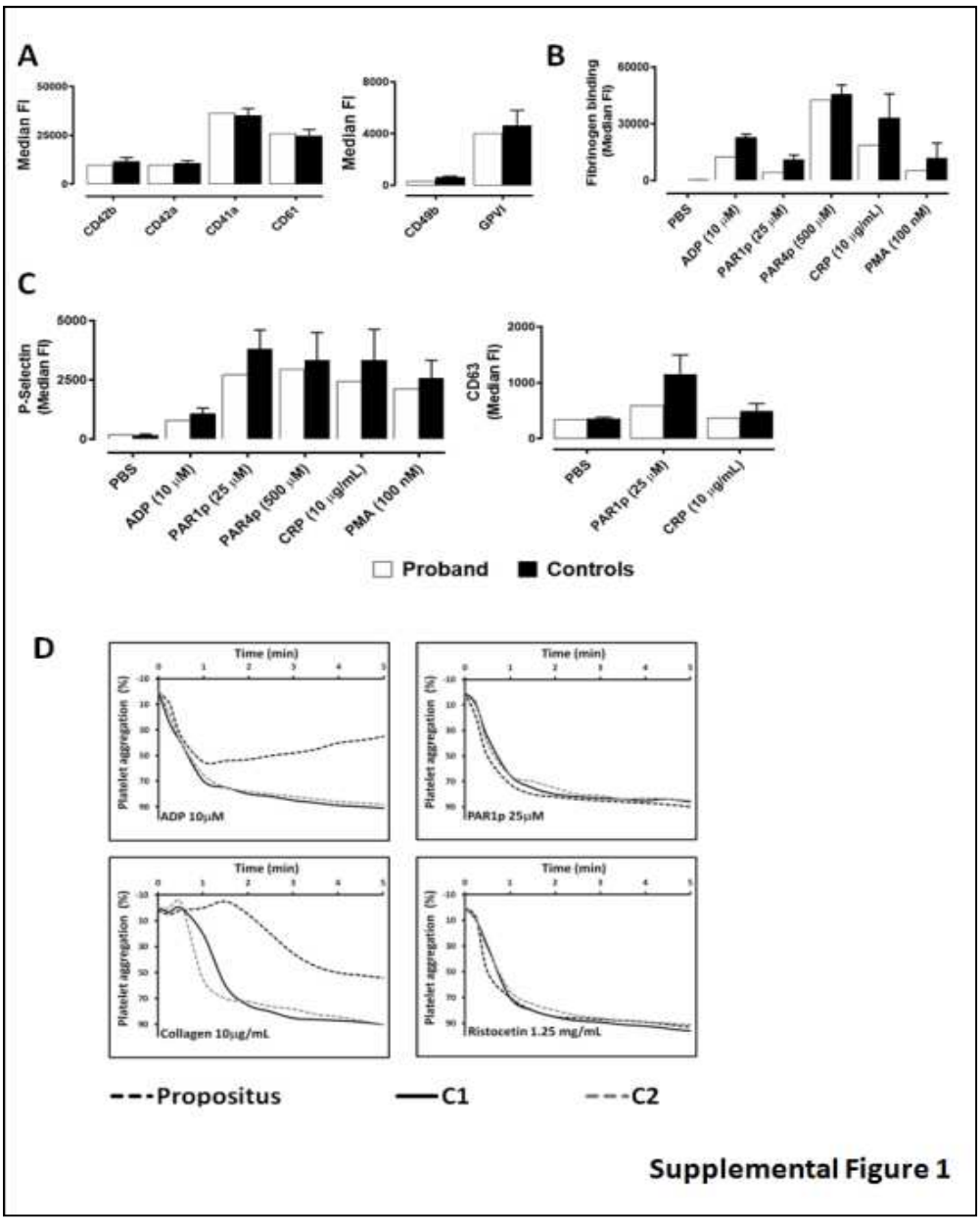

A) GPs expression profiles were assessed by flow cytometry in diluted whole blood from the proband and healthy controls (n=2) assayed in paralel. The fluorescently labelled antibodies used are reported in Supplemental Material. Platelets were incubated under static conditions in the presence of PBS or platelet agonists and of fibrinogen-Alexa 488 **(B)**, anti-CD62P or CD63 monoclonal antibodies **(C),** to evaluate fibrinogen binding and the release of α–and δ–granules, respectively, by flow cytometry. In A-C graphs the median fluorescence intensity is shown; mean ± SD of values in the two controls. **D)** Platelet aggregation in response to the indicated agonists was evaluated in PRP from the index case and two healthy controls (C1 and C2)

Supplemental Figure 2: Thromboxane A_2 release in platelet-rich-plasma and eicosanoid production in whole blood from the proband and time-matched controls.

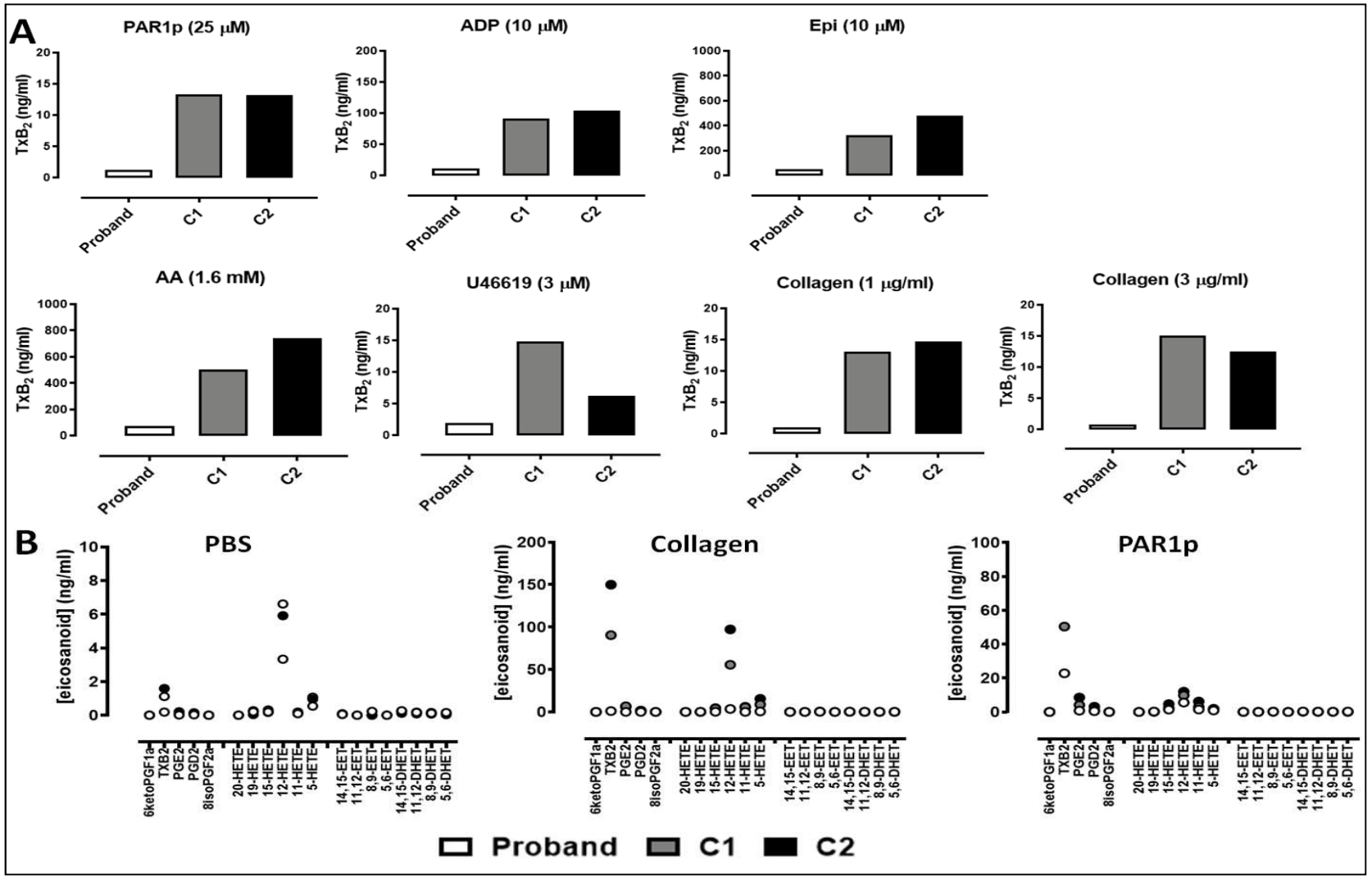

A) TXB_2 levels (ng/mL) in supernatants of platelet aggregation reactions from the proband and time-matched controls (C1 and C2) measured by ELISA. **B)** Eicosanoid levels determined by LC-MS in the proband and controls (C1 and C2) whole blood, at basal level (PBS) and following incubation with collagen (30 mg/mL) or TRAP-6 amide (30 µmol/L).

Supplemental Figure 3. Schematic representation for the conservation of the Asn143 N-glycosylation residue in the Cox-1 sequence and its location in the COX-1 tridimensional structure.

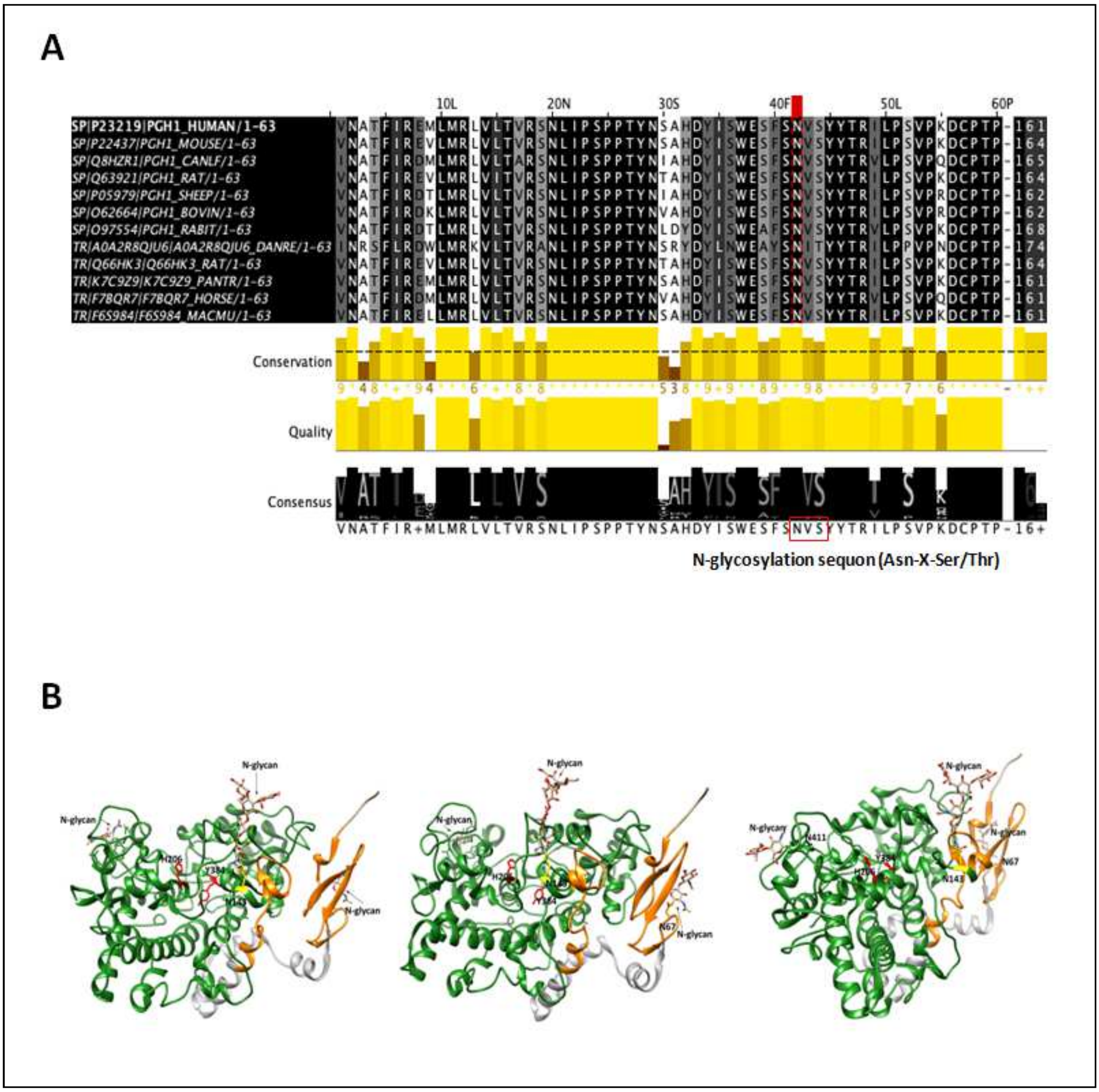

A) Amino acid sequence alignment of COX-1 from different species is represented and the mutated residue (in a red square) is conserved among species. The affected sequence is also highlighted. **B)** The tridimensional structure of human wild-type COX-1 protein was visualized by using the crystal by *Scilimati A et al* (PDB:6y3c) (results to be published) in the Quimera software. N-glycosylation residue 143 is shown in yellow; catalytic resides Y384, H205 are shown in red; glycans are marked with arrows; different domains of COX-1 are coloured with the same pattern used in panel A.

Supplemental Figure 4: Immunofluorescence analysis of COX-1 in platelets and leukocytes from the patient with the novel *PTGS1* variant p.Asn143S and time-matched control.

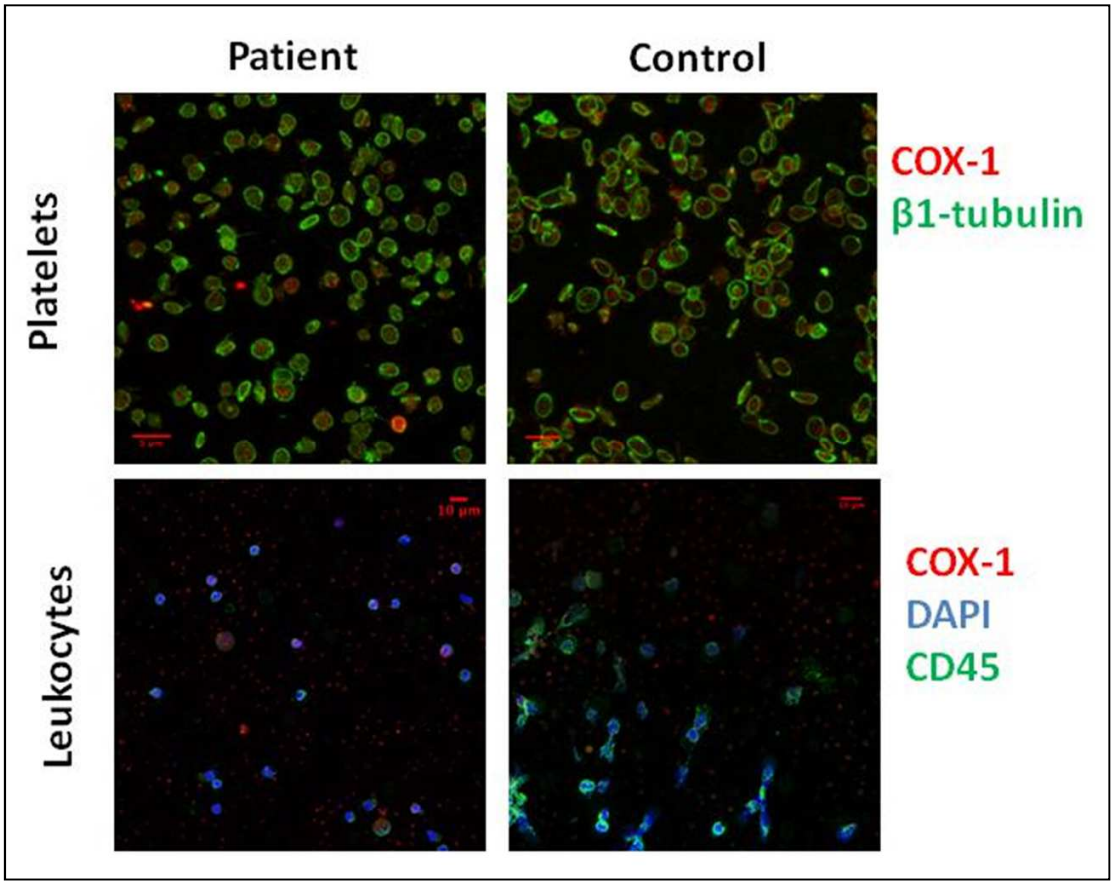

In platelets tubulin is represented in green and COX-1 in red. Leukocytes were identified using CD45 (green), as surface marker, and DAPI (blue) as a nuclear marker, while COX-1 is represented in red. Images were acquired with Airyscan laser scanning confocal microscope. Bars represent 5 μm for platelets and 10 μm for leukocytes.

Supplemental Figure 5. The Ser143 COX-1 mutant has a dominant-negative effect on the enzymatic activity of native COX-1.

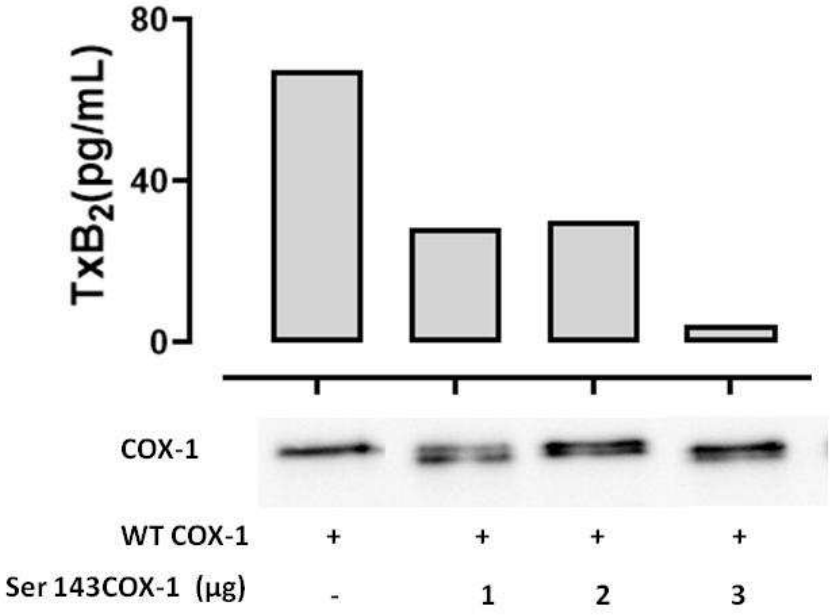

HEK 273 cells were transfected with vector expressing wild-type Asn143 COX-1 and the neomicine resistance gen and grown in the presence of geneticine. Resistant and stable transfected cell clones were isolated and then transfected with different amounts of Ser143 mutant COX-1. Cells were washed and splitted for preparation of protein lysates and for AA (500uM) stimulation and TXA_2 production measurement by ELISA. A double COX-1 protein is seen in co-transfected cells.

Supplemental Table 1. Blood parameters and clinical bleeding symptoms in the heterozygous carrier of the novel variant p.Asn143Ser in COX-1

Age	**13 yr**
Blood Parameters	
WBC, $\times 10^9$/L	5.73
RBC, $\times 10^{12}$/L	3.89
Hb, g/dL	12.2
Hct (%)	33.3
Platelets, $\times 10^9$/L	206
MPV, fL	11.4
PFA-100 CT (s)	
Collagen/epinephrin	>300
Collagen/ADP	120s
ISTH-BAT score	6
Bleeding symptoms	-Epistaxis -Easy bruising and petechiae -Menorrhagia -Bleeding after surgery

WBC=white blood cells; RBC=red blood cells; Hb=hemoglobin; Hct=hematocrit; MPV=mean platelet volume; PFA-100= platelet function analyzer; CT=closure times. ISTH-BAT: International Society on Thrombosis and Haemostasis –Bleeding Assessment tool.

Supplemental Table 2. Agonist-induced eicosanoid production in whole blood determined by LCMS. Total eicosanoid levels in whole blood from healthy controls (C1 and C2) or from the proband following incubation with vehicle (PBS), collagen (30 µg/mL) or PAR1p (TRAP-6 amide) (25 µM).

Metabolite (ng/mL)	Patient			C1			C2		
	PBS	Collagen (30 µg/mL)	PAR1p (25µM)	PBS	Collagen (30 µg/mL)	PAR1p (25µM)	PBS	Collagen (30 µg/mL)	PAR1p (25µM)
6ketoPGF1a	0.00100	0.00367	0.00267	0.00500	0.01533	0.00200	0.00100	0.00867	0.02033
TXB2	0.19000	0.98600	22.79667	1.11633	90.45033	50.41900	1.58400	149.89300	113.25867
PGE2	0.01433	0.03200	0.76033	0.07967	6.74867	4.09833	0.20433	5.82600	8.49033
PGD2	0.02833	0.04367	0.43700	0.09233	1.48867	0.94333	0.14533	1.38967	3.12333
8isoPGF2a	0	0	0	0	0	0	0	0	0
20-HETE	0	0	0	0	0	0	0	0	0
19-HETE	0.20600	0.23233	0.19600	0.26467	0.12200	0.16300	0.04067	0.10967	0.10767
15-HETE	0.19500	0.16033	1.40067	0.30800	3.98867	2.41967	0.17133	4.51300	4.63833
12-HETE	3.33033	3.48100	5.57833	6.61000	55.63067	9.77867	5.91767	97.24267	11.97133
11-HETE	0.09600	0.11467	1.45267	0.18567	5.41400	2.99200	0.10700	6.09967	6.19967
5-HETE	0.54433	0.57367	0.88733	1.07233	8.84433	1.53967	0.95200	15.41467	1.88433
14,15-EET	0.05000	0.06333	0.06267	0.04800	0.03600	0.04667	0.09200	0.05167	0.00000
11,12-EET	0	0	0	0	0	0	0	0	0
8,9-EET	0.22833	0.28867	0.13033	0.00000	0.41633	0.22267	0.00000	0.34500	0.08933
5,6-EET	0	0	0	0	0	0	0	0	0
14,15-DHET	0.26433	0.24933	0.25900	0.24867	0.20900	0.20033	0.11800	0.12733	0.13867
11,12-DHET	0.17167	0.13200	0.15500	0.18000	0.14700	0.15667	0.08467	0.09167	0.10200
8,9-DHET	0.12233	0.14967	0.15133	0.16567	0.12000	0.10433	0.07133	0.04400	0.06967
5,6-DHET	0.15633	0.15467	0.19933	0.13933	0.11067	0.12000	0.03800	0.04167	0.06200

Supplemental Table 3. ACMG classification (A) and pathogenicity scores (B) of the p.Asn143Ser variant through different predictors.

A

Verdict: ***"Uncertain Significance"***

X PVS1	X PS1	X PS2	X PS3	☐ PS4	X PM1	√ PM2 Moderate	☐ PM3
X PM4	X PM5	X PM6	X PP1	X PP2	√ PP3 Supporting	☐ PP4	X PP5
X BA1	X BS1	X BS2	X BS3	X BS4			
√ BP1 Supporting	☐ BP2	X BP3	X BP4	☐ BP5	X BP6	X BP7	

B

Computational predictor	Classification	Score
MutationTaster	Disease causing	1
Mutation assessor	Medium	3.46
FATHMM	Tolerated	2.31
FATHMM-MKL	Damaging	0.9959
FATHMM-XF	Damaging	0.9037
LRT	Deleterious	0
DEOGEN2	Tolerated	0.4877
EIGEN	Pathogenic	0.9345
EIGEN PC	Pathogenic	0.8692
SIFT	Damaging	0.002
SIFT4G	Damaging	0.004
PROVEAN	Damaging	-4.22
MVP	Benign	0.8289
REVEL	Benign	0.546
PrimateAI	Damaging	0.4489
MetaSVM	Tolerated	-0.6806
MetaLR	Tolerated	0.1654
Polyphen	Probably damaging	0.997
Allele frequency	Not reported previously	

ACMG=American College of Medical Genetics; Allele frequency in general population gnomAD browser database (https://gnomad.broadinstitute.org/); All the information is available on the web tool (https://varsome.com/)

Supplemental Table 4. Flow cytometry determination of COX-1 expression in HEK 293 T cells transfected with wild-type COX-1 [Asn143], mutant Ser143 or Ala145 COX-1 vectors or co-transfected with wild-type and mutant Ser143 COX-1 vectors [Asn143+Ser143].

	% +α-DYKDDDDK cells	
	MEAN	SD
Asn143	48.04	13.06
Ser143	50.89	8.18
Asn143+Ser143	45.76	14.07
Ala145	49.5	5.93

HEK 293 T cells (2 x 10^5 /well) were transiently transfected with vectors expressing wild-type or mutant COX-1 using Lipofectamine 3000. Comparable transfection efficiencies in either condition were ensured by flow cytometry measurement of intracellular levels of recombinant COX-1 using the BD IntraSure kit (BD Biosciences) and the antibody α-DYKDDDDK*PE. Data show mean % of cell expressing the enzyme.